Holmboe instability in non-Boussinesq fluids

Ricardo Barros and Wooyoung Choi

Citation: Phys. Fluids **23**, 124103 (2011); doi: 10.1063/1.3670611

View online: http://dx.doi.org/10.1063/1.3670611

View Table of Contents: http://pof.aip.org/resource/1/PHFLE6/v23/i12

Published by the American Institute of Physics.

Holmboe instability in non-Boussinesq fluids

Ricardo Barros[1] and Wooyoung Choi[2]
[1]Instituto Nacional de Matemática Pura e Aplicada, Rio de Janeiro, RJ 22460-320, Brazil
[2]Department of Mathematical Sciences, New Jersey Institute of Technology, Newark, New Jersey 07102-1982, USA and Division of Ocean Systems Engineering, Korea Advanced Institute of Science and Technology, Daejeon 305-701, Korea

(Received 1 January 2011; accepted 14 August 2011; published online 22 December 2011)

We perform the stability analysis for stratified shear flows whose density transition layer is much thinner than, and possibly, displaced with respect to, the velocity shear layer for which Holmboe instability along with the well-known Kelvin-Helmholtz (KH) instability is known to be present. Here, we provide a more complete picture of stability characteristics of stratified shear flows with taking into account the effects of non-negligible density increment for which the classical Boussinesq approximation is no longer valid. It is shown that, in addition to the Kelvin-Helmholtz and Holmboe instabilities for which two unstable modes exist, there is another instability with a single unstable mode so that the unstable waves excited by this instability mechanism propagate only in one direction. Depending on the physical parameters, this unstable mode may not be captured by the stability analysis under the Boussinesq approximation. With a better understanding of the instability mechanisms with including the non-Boussinesq effects, we could validate some of previous experimental results and provide new evidences to observations that have not been fully explained. The results are also expected to be useful in designing laboratory experiments to observe Holmboe waves and estimating their wavelengths and phase speeds. © *2011 American Institute of Physics*. [doi:10.1063/1.3670611]

I. INTRODUCTION

There has been an active search towards the understanding of the generation of turbulence and mixing in density-stratified flows since the pioneering works of Taylor[1] and Goldstein[2] on the stability of stratified shear flows. When the thickness of density transition layer between two layers of different constant densities is comparable to the shear layer thickness, only Kelvin-Helmholtz (KH) instability, characterized by billows traveling at approximately the average velocity between the two layers, is expected to occur. However, the stability characteristics of these flows get more complicated when the density transition layer is much thinner than the shear layer.

Holmboe[3] was the first to point out that a second mode of instability should be present when the thickness of density transition layer vanishes. This unstable mechanism consists of two trains of interfacial waves of equal strength that travel at the same speed, but in opposite directions with respect to the mean flow. This theoretical result, known now as Holmboe instability, has been validated numerically by Hazel,[4] Smyth *et al.*,[5] Smyth and Peltier,[6,7] and Alexakis,[8] although very few signs of its existence were found experimentally. Pouliquen *et al.*[9] have made brief observations of such unstable features in a tilting tube experiment (based on the classical work by Thorpe[10] on Kelvin-Helmholtz instability).

Browand and Winant,[11] Koop and Browand,[12] and Lawrence *et al.*[13] have performed mixing layer experiments in search of Holmboe instability, but have found no positive evidences. Instead of Holmboe instability, one-sided instabilities were observed and mixing was confined to one side of the density interface. This is believed to happen because the density interface is generally displaced with respect to the shear layer in mixing layer facilities. For this reason, as pointed by Lawrence *et al.*,[14] mixing layer experiments are not an effective mean of studying Holmboe instability. More recently Holmboe instability was observed successfully in laboratory experiments by Zhu and Lawrence[15,16] and Tedford *et al.*[17] in exchange flows.

In many of these experiments, two fluids of almost the same densities have been used, such as salt water and fresh water. Therefore, for stability analysis, the Boussinesq approximation has usually been adopted under the assumption that the density jump across the interface is small. Furthermore, for simplicity, the velocity profile has often been approximated by a piecewise linear function. Then, the stability characteristics depend on two physical parameters: the Richardson number and the distance between the density interface and the center of the linear shear layer. Although such stability analysis is useful in understanding the experiments where the density jump is really small, it provides only a limited description of instabilities of the stratified shear flow of our interest. In the present study, no assumption is made regarding the density jump, allowing us to go beyond the Boussinesq limit and explore the non-Boussinesq effects by considering the density increment as an additional parameter.

After briefly presenting in Sec. II, the equations for the hydrodynamic stability of an inviscid, incompressible, stratified shear flow, we discuss the Boussinesq limit in the framework of the three-layer configuration originally studied by Taylor and Goldstein, known to be in good agreement with the linearized Euler equations even for large density increments. We show in Sec. III that this no longer holds if considered the two-layer configuration proposed by Holmboe.[3] To examine the experimental results by Lawrence *et al.*,[13] we include in Sec. IV, the effects of the density interface displacement. A correct explanation of the eigenvalue problem is given, including a region containing one single unstable mode, unnoticed previously. The effect of larger variations of density is also considered in this framework and it is shown how contrasting the results relative to the Boussinesq limit can be, even for small density increments.

II. PRELIMINARIES

A. Governing equation and jump conditions at surfaces of discontinuity

The stability of an inviscid, incompressible, stratified shear flow depends upon the vertical variation of density $\rho(z)$ and of the mean horizontal velocity $U(z)$. The behavior of a small two-dimensional, monochromatic disturbance of wave number k and wave speed c is governed[18] by

$$\phi'' + \frac{\rho'}{\rho}\left(\phi' - \frac{U'}{U-c}\phi\right) + \left[-\frac{g\rho'}{\rho(U-c)^2} - \frac{U''}{U-c} - k^2\right]\phi = 0, \tag{1}$$

where the prime indicates differentiation with respect to z, g is the gravitational acceleration, and ϕ is the complex amplitude of the stream function. For certain purposes, it may be convenient to rewrite Eq. (1) as

$$[\rho[(U-c)\phi' - U'\phi]]' - k^2(U-c)\rho\phi - \left(\frac{g\rho'}{U-c}\right)\phi = 0. \tag{2}$$

To simplify the analysis, piecewise linear velocity and piecewise constant density profiles are often adopted so that, in each subdomain where $\rho = \text{constant}$ and $U'' = 0$, Eq. (1) reduces to

$$\phi'' - k^2\phi = 0, \tag{3}$$

whose general solution for an unbounded fluid domain is given by

$$\phi(z) = Ae^{kz} + Be^{-kz}. \tag{4}$$

Then, at $z = z_0$, where $U(z)$, $\rho(z)$, or $U'(z)$ is discontinuous, the continuity of pressure and normal velocity at this surface leads to the jump conditions

$$\left[\!\left[\rho\left[(U-c)\phi' - \left(U' + \frac{g}{U-c}\right)\phi\right]\right]\!\right] = 0, \tag{5}$$

$$\left[\!\left[\frac{\phi}{U-c}\right]\!\right] = 0, \tag{6}$$

respectively. These jump conditions are not only dictated by physics but also built-in mathematically. For instance, Eq. (5) can be obtained by integrating directly Eq. (2) across the discontinuity from $z_0 - \Delta z$ to $z_0 + \Delta z$, and let $\Delta z \to 0$.

B. Boussinesq approximation

Further approximations can be made under the Boussinesq approximation where $\rho'/(k\rho)$ is assumed to be small, but g/kU^2 is $O(k\rho/\rho')$. Then, after dropping the second term proportional to ρ'/ρ, Eq. (1) can be reduced to the so-called Taylor-Goldstein equation (named after Taylor[1] and Goldstein[2])

$$\phi'' + \left[\frac{N^2}{(U-c)^2} - \frac{U''}{U-c} - k^2\right]\phi = 0, \tag{7}$$

where $N(z)$ is the Brunt-Väisälä frequency defined by $N^2(z) = -g(d\rho/dz)/\rho$. This amounts to *considering the effect of the change in density on the potential energy of a given deformation and neglecting its effect on the inertia.*[2] Similarly to what we have done in Eq. (2), we can write the Taylor-Goldstein equation into the equivalent form

$$[(U-c)\phi' - U'\phi]' - g\left(\frac{\phi}{U-c}\right)\frac{1}{\rho}\rho' - k^2(U-c)\phi = 0. \tag{8}$$

For the case of $\rho = \text{constant}$ and $U'' = 0$, Eq. (7) becomes identical to Eq. (3), but its solution is subject to a jump condition different from Eq. (5)

$$[\![(U-c)\phi' - U'\phi]\!] - g\left(\frac{\phi}{U-c}\right)[\![\ln\rho(z)]\!] = 0, \tag{9}$$

which is obtained by integrating Eq. (8) vertically across a surface of discontinuity, while Eq. (6) remains unchanged.

We might also be interested in a particular case when $\rho(z) = \rho_0 + \tilde{\rho}(z)$, where $\tilde{\rho}(z)$ is a small deviation of a constant state ρ_0. We may then write a model asymptotically equivalent to the Taylor-Goldstein equation by approximating the buoyancy frequency $N(z)$ in Eq. (7) by $N_0(z)$ defined by $N_0^2(z) = -g(d\tilde{\rho}/dz)/\rho_0$. By doing so, we can integrate the equation across a discontinuity to obtain a new jump condition

$$[\![(U-c)\phi' - U'\phi]\!] - \frac{g}{\rho_0}\left(\frac{\phi}{U-c}\right)[\![\tilde{\rho}(z)]\!] = 0. \tag{10}$$

This jump condition has been used, for example, by Lawrence *et al.*[13] and many others in their stability analysis.

The aim of this paper is to explore how different the results can be when the stability analysis is not restricted to these special limits. Before going to the two-layer configuration leading to the so-called Holmboe instability, we consider the three-layer problem of Taylor[1] and Goldstein[2] and compare the two approaches (with and without Boussinesq approximation) to the problem.

C. Results by Taylor and Goldstein for a sheared three-layer configuration

When assuming that, in the undisturbed flow, the velocity varies linearly from one constant value to another while the density is discontinuous so that the undisturbed flow can be described as

$$U(z) = \begin{cases} u_1 & \text{if} \quad z > h \\ \dfrac{u_1 z}{h} & \text{if} \quad -h < z < h\,, \\ -u_1 & \text{if} \quad z < -h \end{cases}$$
$$\rho(z) = \begin{cases} \rho_1(1-\varepsilon) & \text{if} \quad z > h \\ \rho_1 & \text{if} \quad -h < z < h\,, \\ \rho_1(1+\varepsilon) & \text{if} \quad z < -h \end{cases} \tag{11}$$

Eq. (2) can be solved explicitly, as shown in Eq. (4). Then, by imposing the jump conditions (5)–(6), the eigenvalue equation is obtained as a quartic equation for the wave speed c. Following Goldstein,[2] we introduce the non-dimensional variables $\xi = c/u_1$ and $\alpha = 2kh$, and the Richardson number defined by

$$J = \varepsilon g h / u_1^2, \tag{12}$$

to write the eigenvalue equation

$$a_0\xi^4 + a_1\xi^3 + a_2\xi^2 + a_3\xi + a_4 = 0, \tag{13}$$

where the real coefficients can be read from Eq. (8) in Ref. 2. Using Fuller's root location criteria[19] (see also Jury and Mansour;[20] Barros and Choi[21]), it can be shown that the flow becomes unstable when the *discriminant* Δ is negative, and it is, therefore, characterized by two real and two complex conjugate values of the form $c = c_{r_1}$, c_{r_2}, and $c_{r_3} \pm i c_i$ in a narrow band on the (α, J)-plane, as shown in Fig. 1 in Goldstein.[2] As a result, there is a single unstable mode with growth rate $\alpha c_i = \alpha \mathrm{Im}(c)$, propagating with speed $c_{r3} = \mathrm{Re}(c)$. Alternatively, four complex solutions could exist for the case of $\Delta > 0$, but this has not been found for Eq. (13).

As pointed out by Goldstein,[2] Eq. (13) is considerably simplified as ε approaches to zero in such a way that the Richardson number J remains finite. This observation is motivated by the fact that both coefficients a_1 and a_3 in

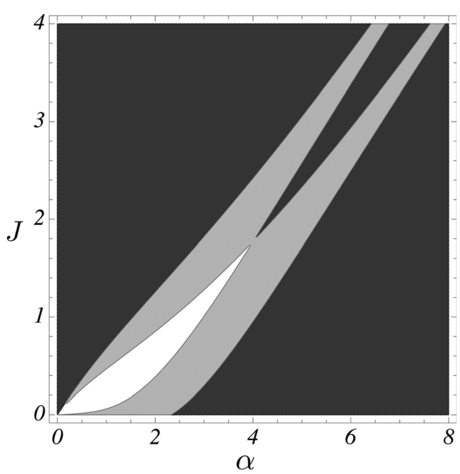

FIG. 1. Stable and unstable regions on the (α, J)-plane for the two-layer configuration with $\varepsilon = 0.5$. The darker shaded region corresponds to the stable region with four real wave speeds. The fluid is unstable elsewhere, being characterized by four complex wave speeds in the white region, and two real and two complex wave speeds in the lighter shaded region.

Eq. (13) are proportional to ε and, therefore, Eq. (13) reduces in this limit to a biquadratic form, which can be solved easily (see Eq. (9) in Ref. 2). Alternatively, this special limit that we will refer to as the *Boussinesq limit* can be obtained with the jump conditions given by Eqs. (6) and (10), instead of Eqs. (5) and (6). As a general property for the biquadratic form obtained in this limit, there exists an unstable mode with wave speed $-c^*$ if c is the complex wave speed of an unstable mode, which we will refer to as *symmetric instabilities*. Since there is, in this case, exactly one unstable mode, the unstable mode has to have a purely imaginary wave speed. As a result, unstable waves for $\varepsilon = 0$ travels at the average velocity between the upper and lower layers, which is 0. For the case of $\varepsilon \neq 0$, it can be shown that unstable waves travel at approximately constant negative speeds, meaning that we can find in both cases, a reference frame relative to which unstable features are *stationary*, which is a signature of the KH instability. Therefore, it can be concluded that Boussinesq and non-Boussineq flows share the common unstable feature (KH instability) in the three-layer configuration discussed in this section.

III. HOLMBOE INSTABILITY IN A TWO-LAYER CONFIGURATION

When the middle density layer collapses to zero thickness from Eq. (11), we then have a two-layer configuration whose stability characteristics are more complicated, as pointed out by Holmboe[3] under the Boussinesq approximation. Here, we explore non-Boussinesq effects that have not been fully described in previous studies. (It was only after submitting this paper that the authors realized that Umurhan and Heifetz[22] have first considered the non-Boussinesq effects in this setting (where the center of the shear layer and the density interface coincide). Some of the results in this section overlap with those presented in Sec. III C in Ref. 22, including Eq. (19).)

Following Holmboe,[3] we consider the following profiles for background density and velocity:

$$U(z) = \begin{cases} u_1 & \text{if} \quad z > h \\ \dfrac{u_1 z}{h} & \text{if} \quad -h < z < h\,, \\ -u_1 & \text{if} \quad z < -h \end{cases}$$
$$\rho(z) = \begin{cases} \rho_1(1-\varepsilon) & \text{if} \quad z > 0 \\ \rho_1 & \text{if} \quad z < 0 \end{cases}. \tag{14}$$

Taking the advantage of the fact that Eq. (1), or Eq. (2), simplifies greatly in each of the four subdomains, we find

$$\phi(z) = \begin{cases} Fe^{-kz} & \text{if} \quad z > h \\ De^{kz} + Ee^{-kz} & \text{if} \quad 0 < z < h \\ Be^{kz} + Ce^{-kz} & \text{if} \quad -h < z < 0 \\ Ae^{kz} & \text{if} \quad z < -h \end{cases}. \tag{15}$$

Then, by imposing the following jump conditions deduced from Eqs. (5) and (6) at $z = \pm h$ and $z = 0$,

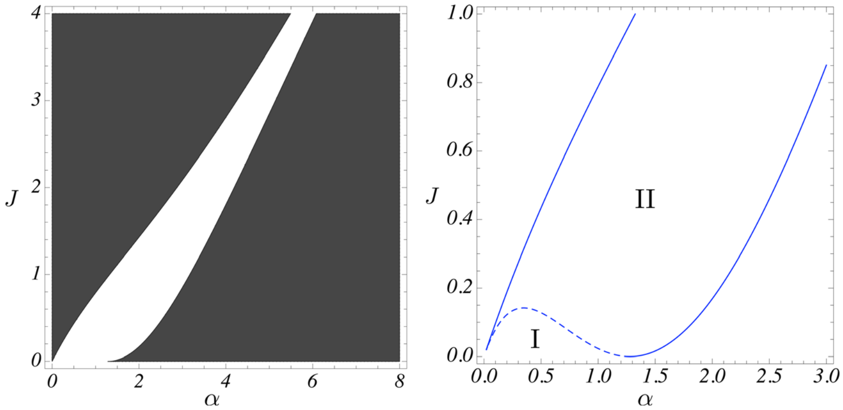

FIG. 2. (Color online) Regions on the (α, J)-plane for stable (shaded region) and unstable (white) symmetric waves in the Boussinesq limit. Also shown on the right-hand side is a close-up view of the curves given by the vanishing of the *discriminant* of Eq. (20). The stability boundaries are indicated by full lines, and the transition between the regions for KH (I) and Holmboe (II) instabilites is indicated by a dashed line.

$$[\![\phi]\!] = 0 \quad \text{at} \quad z = \pm h, \quad z = 0, \tag{16}$$

$$[\![(U-c)\phi' - U'\phi]\!] = 0 \quad \text{at} \quad z = \pm h, \tag{17}$$

$$\left[\!\!\left[\rho\left[(U-c)\phi' - \left(U' + \frac{g}{U-c}\right)\phi\right]\right]\!\!\right] = 0 \quad \text{at} \quad z = 0, \tag{18}$$

we obtain a linear system composed by six equations for the six unknowns. Notice that the continuity of U at $z = \pm h$ and $z = 0$ and the continuity of ρ at $z = \pm h$ have been used to obtain Eqs. (16) and (17), respectively. Straightforward calculations lead to a quartic equation for the dimensionless wave speed $\xi = c/u_1$

$$a_0\xi^4 + a_1\xi^3 + a_2\xi^2 + a_3\xi + a_4 = 0, \tag{19}$$

with its coefficients defined by

$$\begin{aligned}
a_0 &= e^{2\alpha}\alpha^3(2-\varepsilon),\\
a_1 &= 2e^{\alpha}(e^{\alpha}-1)\alpha^2\varepsilon,\\
a_2 &= \alpha\left[\left(e^{2\alpha}(\alpha-1)^2 - 1\right)(\varepsilon - 2) - 2J\alpha e^{2\alpha}\right],\\
a_3 &= -2[e^{\alpha}(\alpha-1)+1]^2\varepsilon,\\
a_4 &= 2J[e^{\alpha}(\alpha-1)+1]^2,
\end{aligned}$$

where the nondimensional parameters α and J are defined as before. When compared with the three-layer configuration discussed previously, the stability diagram for Eq. (19) shows two obvious distinctions (see Fig. 1). The domain of stability is now composed of three distinct regions and a new instability mechanism of different character appears. Namely, instability is no longer equivalent to the condition of $\Delta < 0$, meaning that this physical system allows not only two real and two complex but also four complex wave speeds. For convenience, we will denote by $\mathcal{U}$ the unstable region where $\Delta < 0$.

Before presenting the detailed stability results for non-zero ε, we first discuss briefly the case of $\varepsilon = 0$.

A. Boussinesq limit

For the Boussinesq limit, we proceed as before by taking the limit when ε goes to zero while J remains finite. The quartic equation given by Eq. (19) converts to the biquadratic form

$$e^{2\alpha}\alpha^3\xi^4 - \alpha\left[e^{2\alpha}(\alpha-1)^2 - 1 + J\alpha e^{2\alpha}\right]\xi^2 + J[e^{\alpha}(\alpha-1)+1]^2 = 0, \tag{20}$$

which is equivalent to Eq. (4) found in Lawrence *et al.*[13] Their non-dimensionalization is slightly different from ours and, to recover our result from their expression, it is necessary to replace J by $J/2$. Alternatively, Eq. (20) can be obtained directly by imposing the jump condition under the Boussinesq approximation given by Eq. (10), instead of Eq. (5).

The stable and unstable regions can be depicted on the (α, J)-plane and, when compared with the non-zero ε case (see Fig. 1), two main differences can be noticed. First, there are no signs of the protruding third region of stability for large values of J. Second, the unstable region $\mathcal{U}$ with two real and two complex wave speeds cannot be captured in the Boussinesq limit.

Holmboe[3] was the first to consider this limit and noticed that there should be two distinct mechanisms governing symmetric instabilities. The unstable region is composed of two distinct regions I and II that are separated by a dashed line in Fig. 2. The region I, for smaller Richardson numbers, is characterized by having two pairs of purely imaginary eigenvalues, and it is called the *Kelvin-Helmholtz* mode. Notice that the maximum value of J for which the KH instability can be excited is 0.142 for $0 < \alpha < 1.28$ (see Appendix in Ref. 23). The region II, for larger Richardson numbers, is characterized by having two pairs of conjugate roots of the form $c = \pm c_r \pm ic_i$, and it is known as the *Holmboe* mode, which moves in both directions.

From Fig. 2, the KH instability dominates for J close to 0 while the Holmboe instability dominates when J is greater than 0.142. However, as pointed out by Haigh and Lawrence,[23] it is not obvious from the stability diagram at what value of J there is an actual transition between the two instability mechanisms. In reality, the mode that has a greater growth rate will appear and, therefore, the maximum growth rate for varying J has to be monitored. Fig. 3 shows a (thick solid) curve on the (α, J)-plane along which the maximum growth rates are attained. We can see clearly a discontinuity at $J_T \approx 0.092$ (see Appendix in Ref. 23). This is the critical value of J at which we expect the transition from KH to Holmboe instabilities (equivalently, from two stationary unstable modes with different growth rates to two counter-

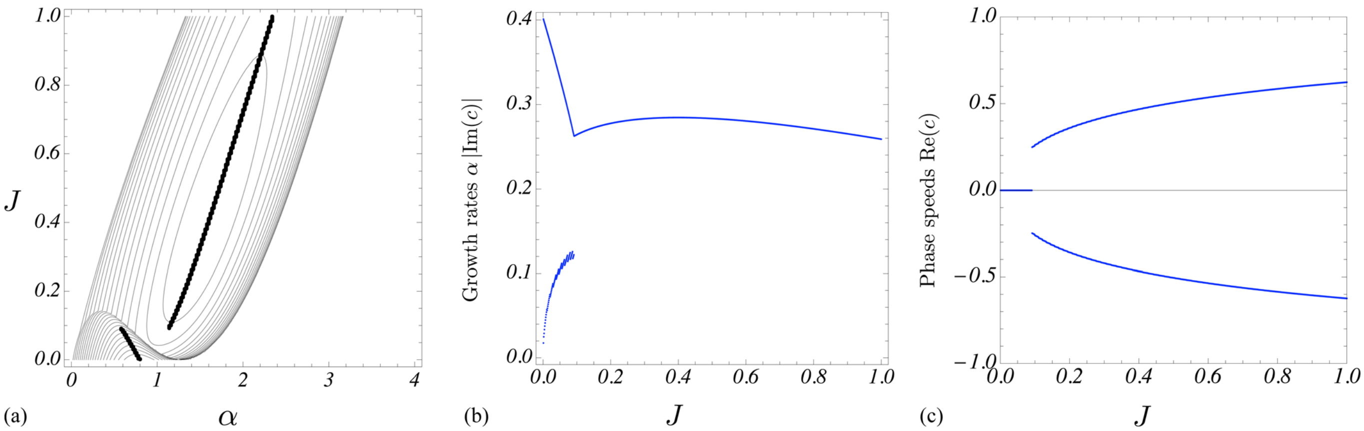

FIG. 3. (Color online) (*a*) Stability diagram on the (α, J)-plane under the Boussinesq approximation with contour lines of constant growth rates (thin lines) and the maximum growth rate curve (thick line). The middle and right-hand side plots, (*b*) and (*c*), respectively, represent the growth rates and phase speeds along the maximum growth rate curve.

propagating unstable modes with same growth rates), as shown in Fig. 3. It is worth noticing that the wave number of the most unstable mode normalized by the shear layer thickness is less than 1 for $J < J_T$ (KH) and greater than 1 for $J > J_T$ (Holmboe).

Figure 4 shows how the KH and Holmboe modes compete as J varies. For $J = 0.08$, the KH mode characterized by zero wave speeds has a higher growth rate than the Holmboe mode, but, as J increases beyond J_T, the Holmboe instability dominates over the KH instability. Eventually, for $J > 0.142$, the Holmboe instability becomes the only unstable mode.

B. The effects of the density increment parameter ε

In order to investigate the non-Boussinesq effects on the instability of a two-layer shear flow, we consider ε as an additional parameter. When compared with the results under the Boussinesq approximation, a good agreement is expected

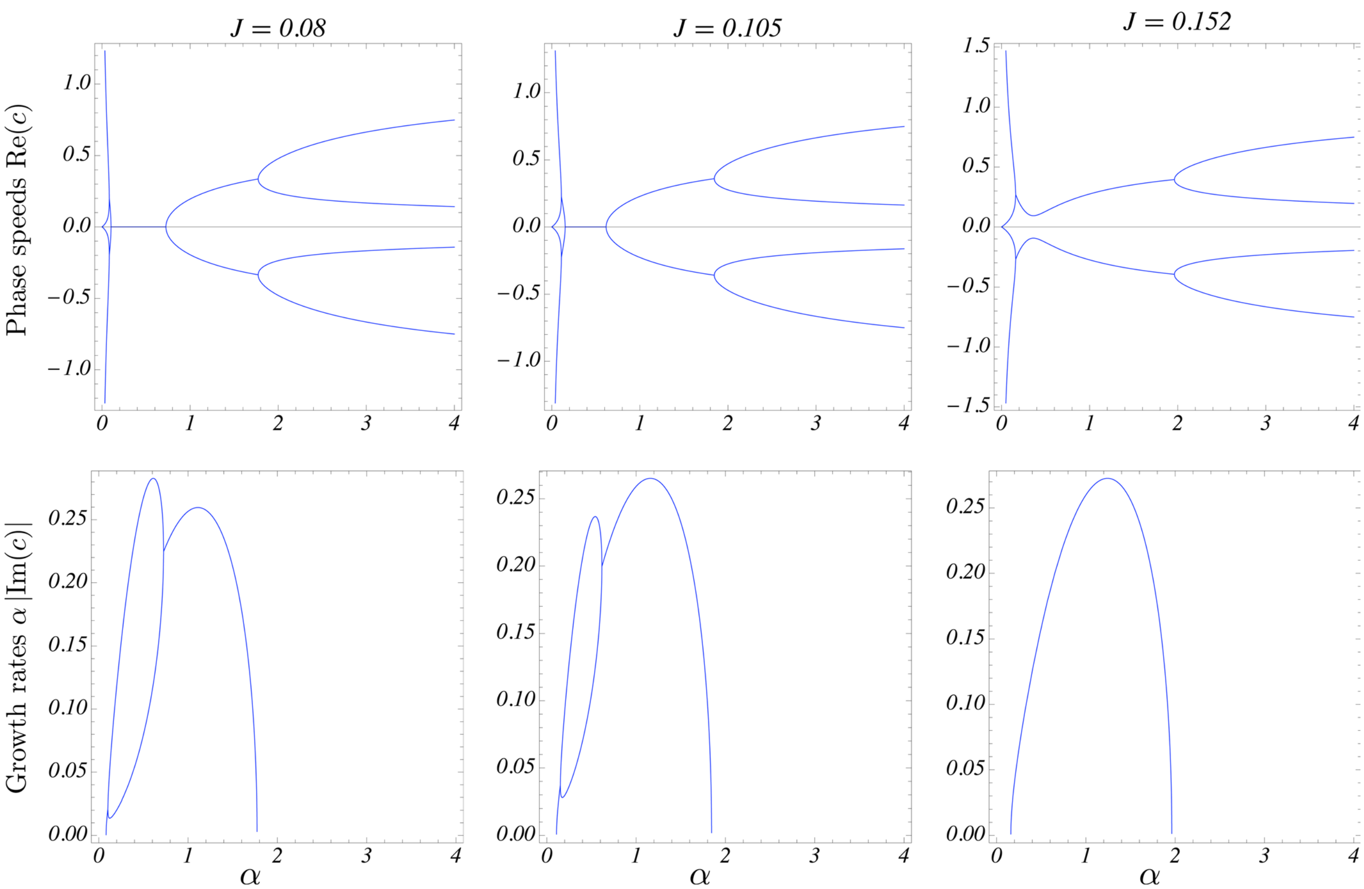

FIG. 4. (Color online) Phase speeds (top panel) and growth rates (bottom panel) for three different Richardson numbers under the Boussinesq approximation. The diagram shows the competition between the KH and Holmboe instability mechanisms for J close to J_T. The former does not manifest for $J > 0.142$.

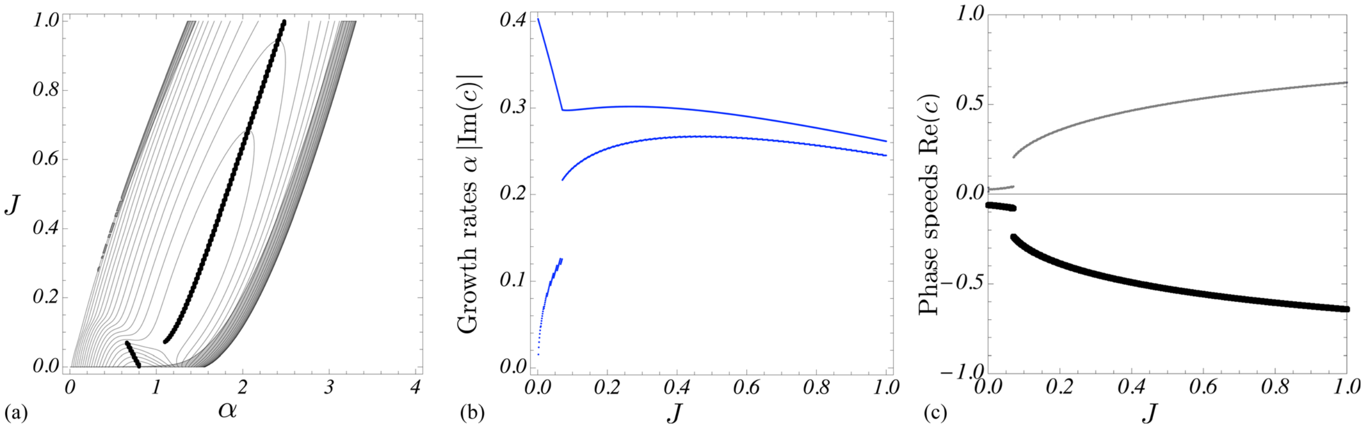

FIG. 5. (Color online) (*a*) Stability diagram on the (α, J)-plane with contour lines of constant growth rates (thin lines) and the maximum growth rate curve (thick line) for $\varepsilon = 0.1$. The shaded region indicates the region $\mathcal{U}$ containing a single unstable mode. The break of symmetry of the flow is well present in the plots for (*b*) the growth rates and (*c*) the phase speeds along the maximum growth rate curve. The dominant unstable mode is represented in (*c*) by a thick line.

for small values of ε. Indeed, as shown in Fig. 5 for $\varepsilon = 0.1$, the stability boundaries do not differ much from those for the Boussinesq case studied by Holmboe (see Fig. 3). By examining the curve on the (α, J)-plane along which the maximum growth rates are attained, we verify that the transition between the two instability modes occurs at $J_T \approx 0.07$, which is smaller than the approximate value of 0.092 for the case of $\varepsilon = 0$.

From Fig. 5, in addition to the critical Richardson number for the transition from the KH instability to the Holmboe instability, it can be seen clearly that the growth rates and the wave speeds of KH and Holmboe instabilities are modified when $\varepsilon \neq 0$. While the growth rate of the KH instability is almost preserved, that of the Holmboe instability is clearly amplified by the density increment in the stratification. The growth rates of the counter-propagating unstable waves excited by the Holmboe instability are no longer the same. This asymmetry prevents the existence of Holmboe waves at exactly same speed for the system, but does not invalidate the existence of two unstable waves traveling in opposite directions (although at different relative speeds), provided that the growth rates of two unstable modes are the same or at least comparable. The term *Holmboe waves* will hereafter be reserved to this special case when two unstable waves with comparable growth rates exist simultaneously and travel in opposite directions.

As mentioned previously, one of unique features that cannot be captured under the Boussinesq approximation is the existence of an unstable region defined by $\Delta < 0$, where only one unstable mode exists. For this particular value of $\varepsilon = 0.1$, we observe that this unstable region that we denote by $\mathcal{U}$ (the shaded regions near the stability boundaries) is rather narrow and it has no influence on the maximum growth rate curve. On the other hand, for large values of ε, the role of the unstable region $\mathcal{U}$ is no longer negligible, as shown in Fig. 6. This could ultimately prevent any possibility for the existence of Holmboe waves for the system (e.g., $\varepsilon = 0.5$).

Figure 6 also reveals that the gap in α at $J = J_T$ on the maximum growth rate curve can be strongly reduced (for $\varepsilon = 0.18$), and even vanish if larger values of ε (for $\varepsilon = 0.3$ and 0.5) are considered. Our numerical results show that the maximum growth rate curve on the (α, J)-plane becomes continuous when $\varepsilon \approx 0.2$, suggesting that a transition from the KH to Holmboe instability is no longer obvious from the maximum growth rate curve. Also evident from the figure is the fact that the difference between the growth rates of two unstable modes traveling in opposite directions tends to increase with ε and the Holmboe instability eventually disappears. Then, we will be left mainly with one-sided instability characterized by a single unstable mode propagating to the left (see the middle panel in Fig. 6) and, in general, we should not expect finding Holmboe instability for an arbitrary range of Richardson number.

IV. LACK OF SYMMETRY DUE TO A DENSITY INTERFACE DISPLACEMENT

Although Holmboe waves have been predicted since 1962, it was not before 1996 that these were actually found in laboratory experiments (Zhu and Lawrence[15]) even if Pouliquen *et al.*[9] had been able to observe the early onset of these instabilities. Before their work, only one-sided instabilities had been observed, which was believed to be a result of the background flow losing its symmetry. As discussed in the preceding section, the break of symmetry arises when taken into account the density increment in the stratification. However, there are at least two other ways for this to happen: adopting a finite-depth configuration with rigid horizontal boundaries placed at different distances from the center of the shear layer,[24,25] or by displacing the density interface away from the middle of shear layer at $z = 0$.[13,24,25] The displaced interface is of particular relevance to earlier experiments since it is found in mixing layer facilities that the density interface is generally displaced from the inflection point for the background velocity. This has been explored by Lawrence *et al.*[13] as a key argument to understand why one-sided instabilities are observed consistently in mixing layer facilities. As explained by Lawrence *et al.*,[14] this asymmetry that can be varied, but not eliminated, is caused by the fact that when the fluids—initially separated by a splitter plate—merge at the trailing edge of the splitter plate, the point of

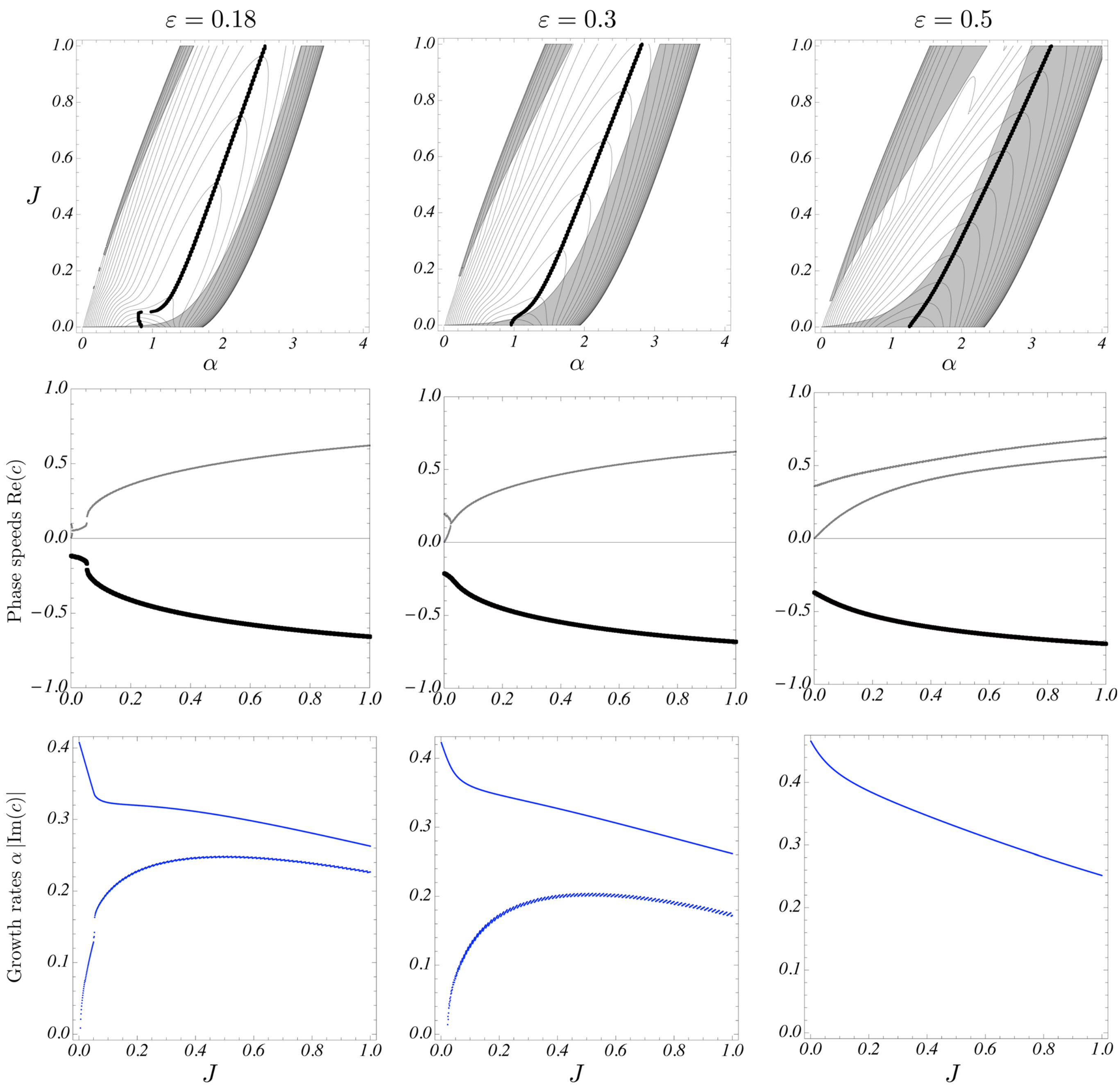

FIG. 6. (Color online) Top panel: Stability diagram on the (α, J)-plane with contour lines of constant growth rates (thin lines) and the maximum growth rate curve (thick line). The corresponding values of phase speeds (middle panel) and growth rates (bottom panel) along the maximum growth rate curve for $\varepsilon = 0.18$, 0.3, and 0.5 (from left to right). The thick lines in the phase speed diagrams represent the dominant unstable mode.

maximum vorticity is found on the high speed side of the density interface. To contemplate this situation, following Lawrence *et al.*,[13] we consider

$$U(z) = \begin{cases} u_1 & \text{if} \quad z > h \\ \dfrac{u_1 z}{h} & \text{if} \quad -h < z < h\,, \\ -u_1 & \text{if} \quad z < -h \end{cases} \qquad (21)$$

$$\rho(z) = \begin{cases} \rho_1(1-\varepsilon) & \text{if} \quad z > -d \\ \rho_1 & \text{if} \quad z < -d \end{cases},$$

where the density interface is placed at the level $z = -d$, with $0 < d < h$. The linear stability analysis leads to a quartic equation for the dimensionless wave speed $\xi = c/u_1$

$$a_0\xi^4 + a_1\xi^3 + a_2\xi^2 + a_3\xi + a_4 = 0, \qquad (22)$$

where the coefficients depend on the wave number α, Richardson number J, and ratio $\delta = d/h$ (see Appendix). When $\delta \neq 0$, coefficients a_1 and a_3 are no longer proportional to ε. Therefore, even in the limit case when ε goes to zero, we should not expect to bring the quartic equation down to a biquadratic form (see Eq. (3) in Ref. 13).

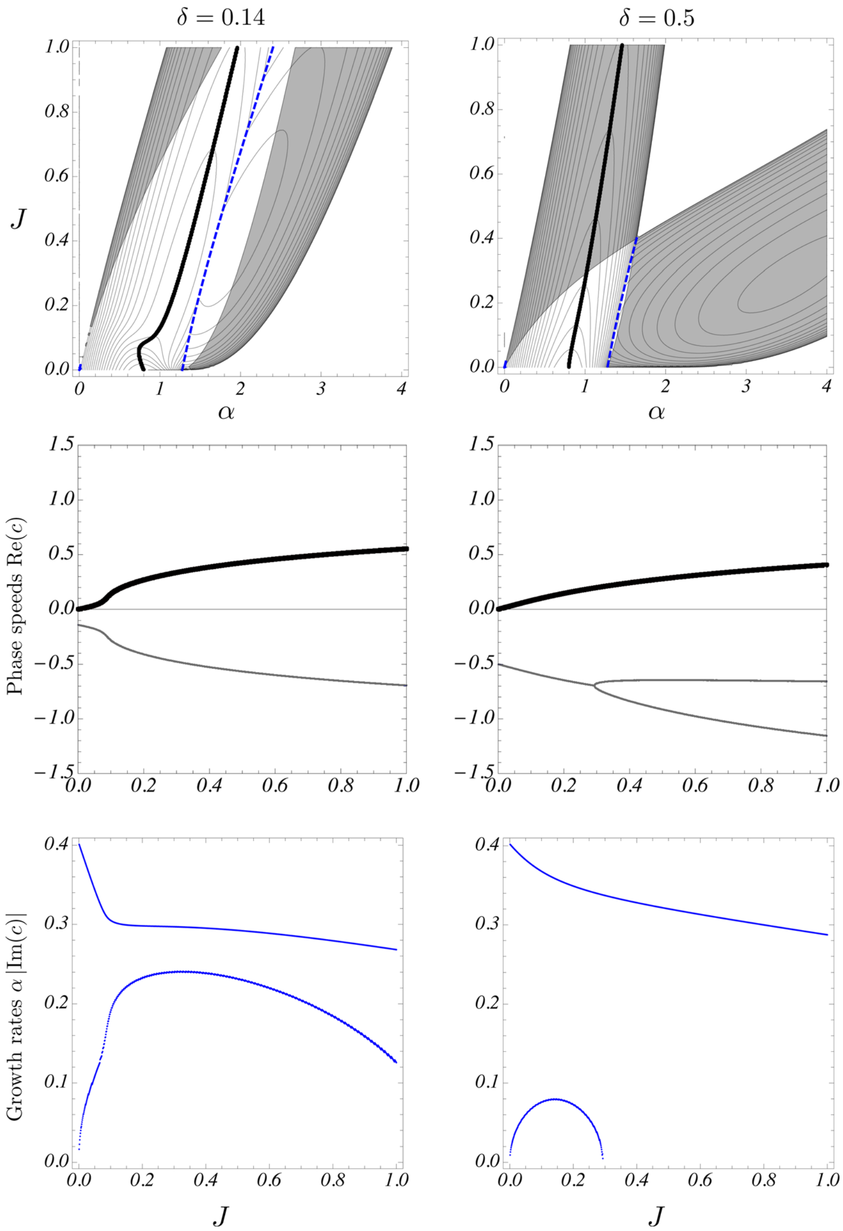

FIG. 7. (Color online) Top panel: Stability diagram on the (α, J)-plane with contour lines of constant growth rates (thin lines) and the maximum growth rate curve (thick line). The corresponding values of phase speeds (middle panel) and growth rates (bottom panel) along the maximum growth rate curve. The thick lines in the phase speed diagrams represent the dominant unstable mode. In both situations, the density increment parameter is $\varepsilon = 4 \times 10^{-4}$, and we have considered $\delta = 0.14$ (left-hand side) and $\delta = 0.5$ (right-hand side). The curve along which true Holmboe waves exist is indicated by a dashed line at the stability diagrams.

To isolate the effects of δ, we first consider the physical parameters used in the experiments conducted by Lawrence *et al.*,[13] where $\delta = 0.5$ and the modified gravitational acceleration $g'(=g\varepsilon)$ is $0.4\,\mathrm{cm/s^2}$, which yields $\varepsilon \approx 4 \times 10^{-4}$. For this value of ε, the Boussinesq approximation should be perfectly valid and the effects of ε should be negligible. The effect of δ on the stability diagram is remarkable when Fig. 7 is compared with Fig. 3. In particular, the unstable region $\mathcal{U}$ plays an important role, but its existence presumably has been unnoticed so far. For example, the following property has often been used in the literature (see the right-bottom of page 2362 in Ref. 13)

$$c_r^+ + c_r^- = \delta, \tag{23}$$

that would hold for Eq. (22) with $\varepsilon = 0$, provided that we divide the equation by a_0 and assume the existence of four complex wave speeds written as $c = c_r^+ \pm i c_i^+, c_r^- \pm i c_i^-$. However, the last assumption is not valid everywhere in the region of instability, since $\mathcal{U}$ is a non-empty set, and so there are solutions of the form $c = c_{r_1}, c_{r_2}$, and $c_{r_3} \pm i c_i$, for which

$$c_{r_1} + c_{r_2} + 2c_{r_3} = 2\delta. \tag{24}$$

This implies that, although Lawrence *et al.*[13] have used values of J as large as 0.6 to seek Holmboe waves experimentally, no Holmboe waves were to be seen as soon as the maximum growth rate curve enters this region $\mathcal{U}$ (about $J \approx 0.293$).

Even for smaller values of J for which the linear stability analysis for $\delta = 0.5$ predicts two unstable modes, the difference between their growth rates is so large that one mode is always dominant and, as a result, the two unstable modes can hardly be excited simultaneously. Furthermore, the dominant mode always propagates to the right (see the middle panel in Fig. 7). The linear stability analysis provides a good explanation for the observed one-sided instabilities in experiments, but not everything can be effectively explained by

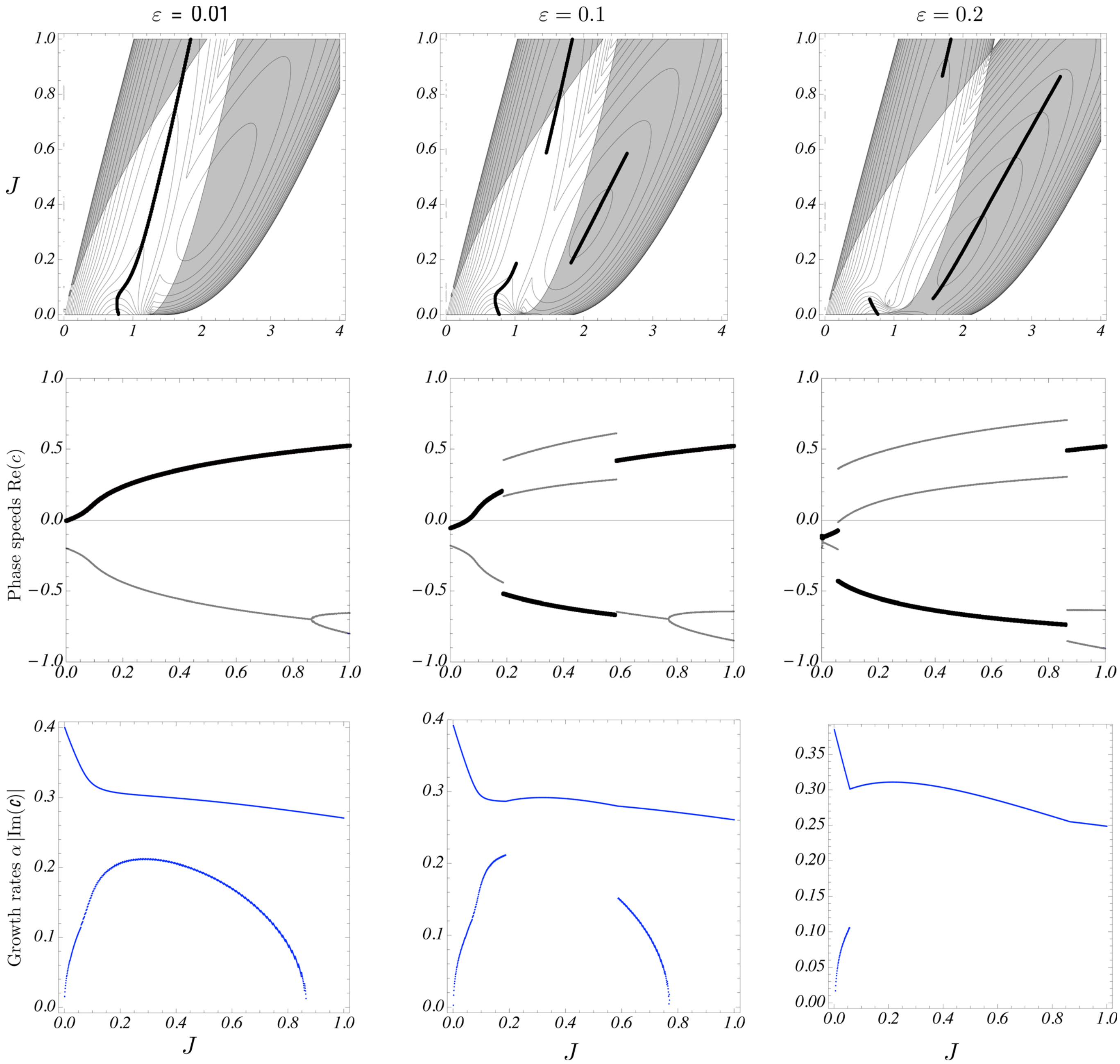

FIG. 8. (Color online) Top panel: Stability diagram on the (α, J)-plane with contour lines of constant growth rates (thin lines) and the maximum growth rate curve (thick line). The corresponding values of phase speeds (middle panel) and growth rates (bottom panel) along the maximum growth rate curve. The thick lines in the phase speed diagrams represent the dominant unstable mode. The value of δ is fixed at 0.2 and different values of ε are considered: $\varepsilon = 0.01$, 0.1, and 0.2 (from left to right).

using this linear analysis. Experimentally, Lawrence *et al.*[13] have detected different nonlinear responses of the flow to the instability about $J = 0.2$; more precisely, for Richardson numbers greater than 0.2, they have observed the formation of cusps protruding into the dominant layer, whereas a series of vortex tubes resembling the Kelvin-Helmholtz billows were observed for Richardson numbers less than 0.2. Although Carpenter *et al.*[26] recently examined a criterion on the formation of cusps using linear theory, it is non-trivial to obtain such information from the linear stability diagram. Furthermore, nonlinearity should play a role in the further development of linearly unstable waves, which is beyond the scope of the present study.

So far, we have been examining the unstable features along the maximum growth rate curve. Let us forget the maximum growth rate curve for a moment and investigate from a mathematical point of view if "true" Holmboe waves can exist for the system even when $\delta = 0.5$. Here, we define the true Holmboe waves as two unstable waves with exactly same growth rates. For simplicity, divide Eq. (22) by a_0 (with $\alpha \neq 0$) and write

$$\xi^4 + \widetilde{a}_1\xi^3 + \widetilde{a}_2\xi^2 + \widetilde{a}_3\xi + \widetilde{a}_4 = 0, \qquad (25)$$

with $\widetilde{a}_i = a_i/a_0$. Assume that the solutions for true Holmboe waves can be written as $c = c_{r_1} \pm ic_i$ and $c_{r_2} \pm ic_i$. Viète's formulas lead to

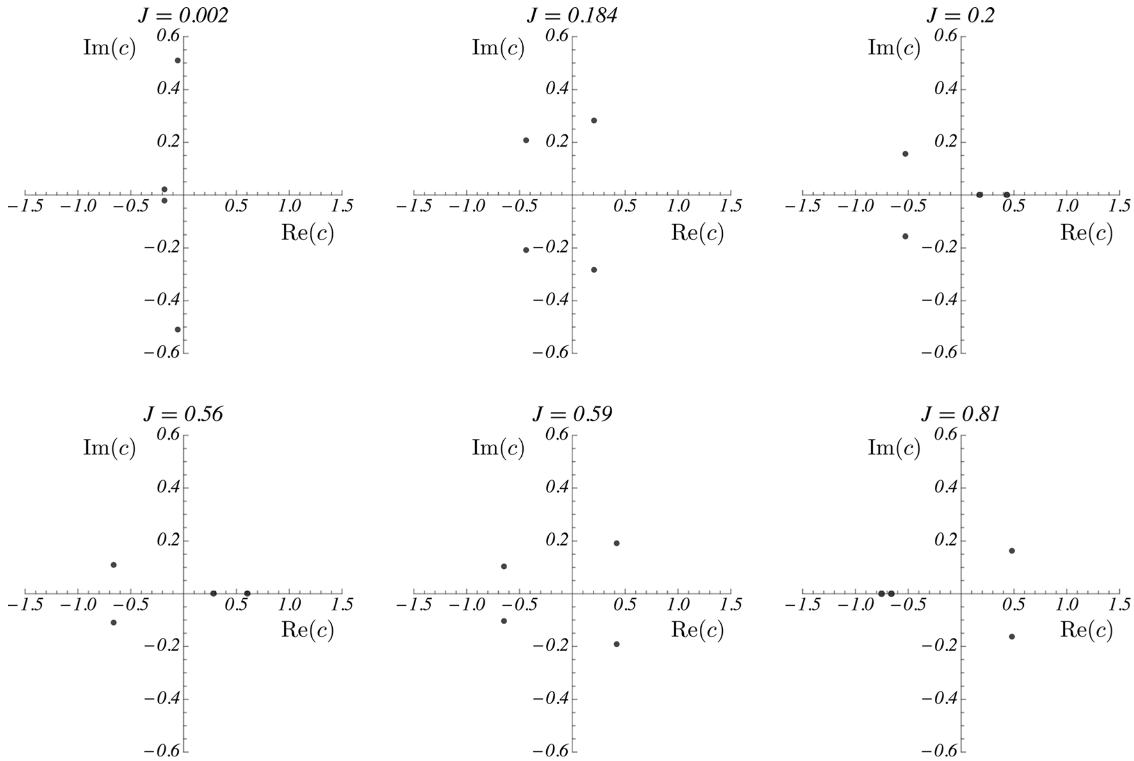

FIG. 9. Evolution of the eigenvalues along the maximum growth rate curve for $\delta = 0.2$ and $\varepsilon = 0.1$.

$$2s = -\widetilde{a}_1, \quad s^2 + 2\left(p + c_i^2\right) = \widetilde{a}_2,$$
$$2\left(p + c_i^2\right)s = -\widetilde{a}_3, \quad \left(p - c_i^2\right)^2 + s^2 c_i^2 = \widetilde{a}_4, \tag{26}$$

where s and p are defined by the sum and product of the real parts of the solutions, respectively, as $s = c_{r_1} + c_{r_2}$ and $p = c_{r_1} c_{r_2}$. Provided that $\widetilde{a}_1 \neq 0$ (which is true for $\alpha > 0$ and $\varepsilon > 0$), this overdetermined system can be solved under an implicit relation of the form

$$\widetilde{a}_1{}^3 - 4\widetilde{a}_1\widetilde{a}_2 + 8\widetilde{a}_3 = 0, \tag{27}$$

constrained by

$$\left(\widetilde{a}_2 - \frac{1}{4}\widetilde{a}_1{}^2\right)^2 - 4\widetilde{a}_4 < 0. \tag{28}$$

Surprisingly, both conditions (27) and (28) can be satisfied regardless of the values of δ and ε considered, and the result is displayed as a dashed line on the (α, J)-plane in Fig. 7. It can be seen that, for $\delta = 0.5$, true Holmboe waves are considerably weaker than the instabilities along the maximum growth rate curve, and for this reason, we do not expect them to be particularly relevant from an experimental point of view.

For small values of δ relevant for the asymmetric profile far downstream of the splitter plate, we are close to the original symmetric case and, as a result, we would expect to observe Holmboe waves. However, this phenomenon has not been well documented.[14] This may be related to the fact that, even if δ is reduced, in general, we cannot expect to observe Holmboe waves for an arbitrary range of Richardson numbers, as discussed earlier in Sec. III B for the non-displaced case (see Fig. 6). For example, we assume that we conduct an experiment with $\delta = 0.14$. When we compute the relative difference σ_{diff} between the growth rates of unstable modes along the maximum growth rate curve defined by

$$\sigma_{\text{diff}} = \frac{|\alpha c_{i_1} - \alpha c_{i_2}|}{\min\limits_{k=1,2}\{\alpha c_{i_k}\}}, \tag{29}$$

we can see that, to observe Holmboe waves, the Richardson number has to be chosen to be $J \approx 0.345$ (see Fig. 7) for which the relative difference attains its minimum (≈ 0.229). If J is far different from this value, one growth rate is much greater than the other and, therefore, only one unstable mode would be excited experimentally. How close the growth rates of two unstable modes have to be so that both unstable modes are excited simultaneously is something that deserves further investigation, including the effect of nonlinearity.

A. The effects of larger values of ε

We explore here the non-Boussinesq effects with considering larger values of ε in the case when the interface is displaced with respect to the shear layer. In Fig. 8, we increase the value of ε up to 0.2 with a fixed value of $\delta = 0.2$. For a small value of $\varepsilon = 0.01$, the results follow very closely those obtained for $\varepsilon = 0$, but distinct features can already be perceived for $\varepsilon = 0.1$. The maximum growth rate curve on the (α, J)-plane is no longer continuous; discontinuities occur twice (for $J \approx 0.186$ and 0.586), as shown in Fig. 8. Remarkably, these discontinuities are not associated to a transition from KH to Holmboe instability, which has been often observed in the non-displaced case ($\delta = 0$). As shown in Fig. 9, at the first discontinuity, there is a passage from the

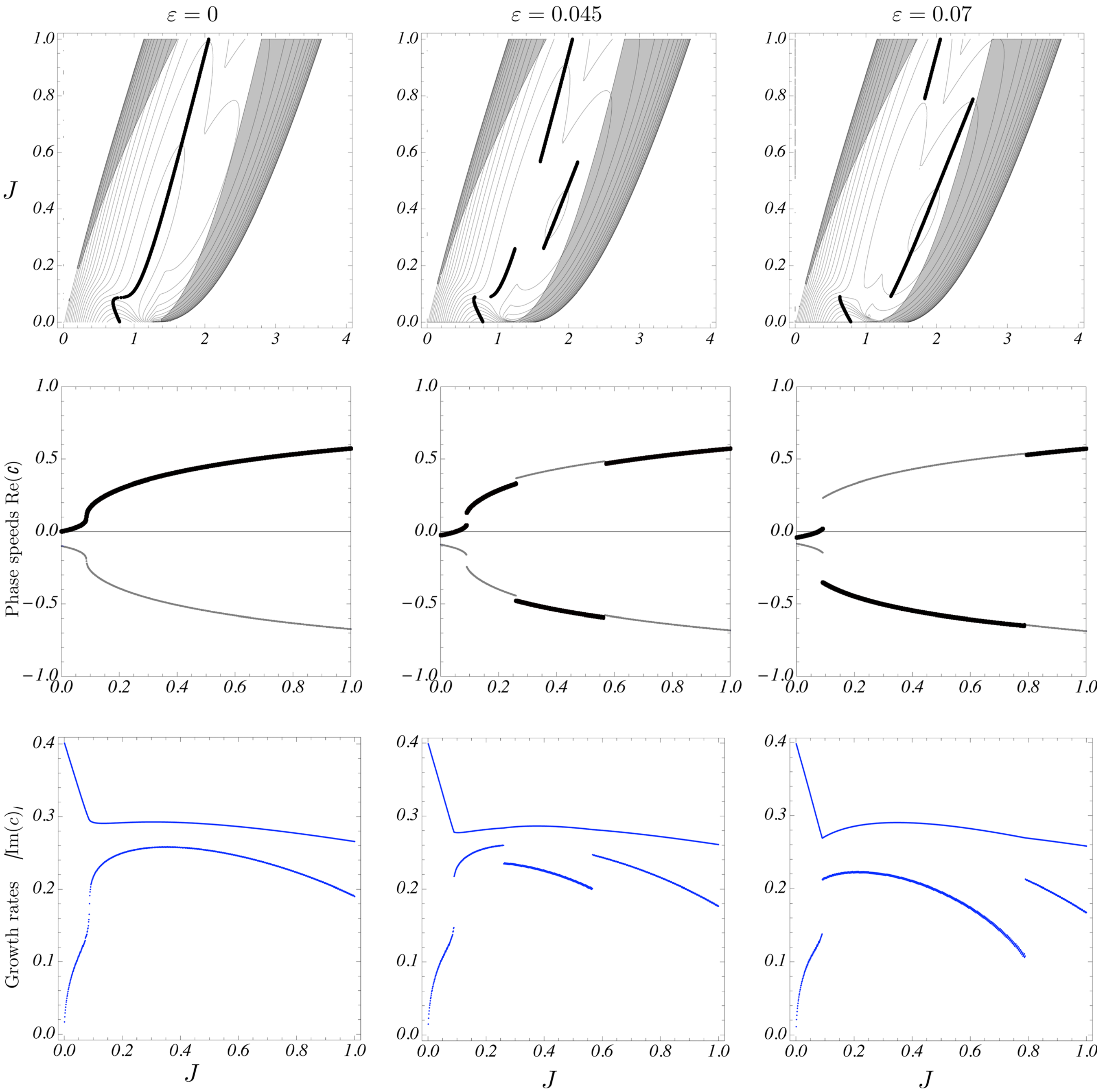

FIG. 10. (Color online) Top panel: Stability diagram on the (α, J)-plane with contour lines of constant growth rates (thin lines) and the maximum growth rate curve (thick line). The corresponding values of phase speeds (middle panel) and growth rates (bottom panel) along the maximum growth rate curve. The thick lines in the phase speed diagrams represent the dominant unstable mode. The value of δ is fixed at 0.1 and different values of ε are considered: $\varepsilon = 0$, 0.045, and 0.07 (from left to right).

unstable region (in white) with four complex wave speeds to the region $\mathcal{U}$, where only two wave speeds are complex, associated to a transition from the right-going waves (in the case when the relative difference σ_{diff} is too large) to the left-going waves. At the second discontinuity, the reverse situation takes place. This process evolves as ε increases up to the point where the maximum growth rate curve is entirely included in the region $\mathcal{U}$. As a final remark, it is worth emphasizing that the maximum growth rate decreases as ε increases, which is contrary to the case when $\delta = 0$.

B. In search of Holmboe waves

We intend with this work to bring attention to the importance of taking into account the density increment in the stratification in excitation of Holmboe waves. From the examples described above, we notice that the values of ε should be order of magnitude of 10^{-1} to see any major difference from the case of $\varepsilon = 0$. To our knowledge, no experiments towards the search of Holmboe waves were conducted with values of ε this large; for instance, Lawrence *et al.*[13]

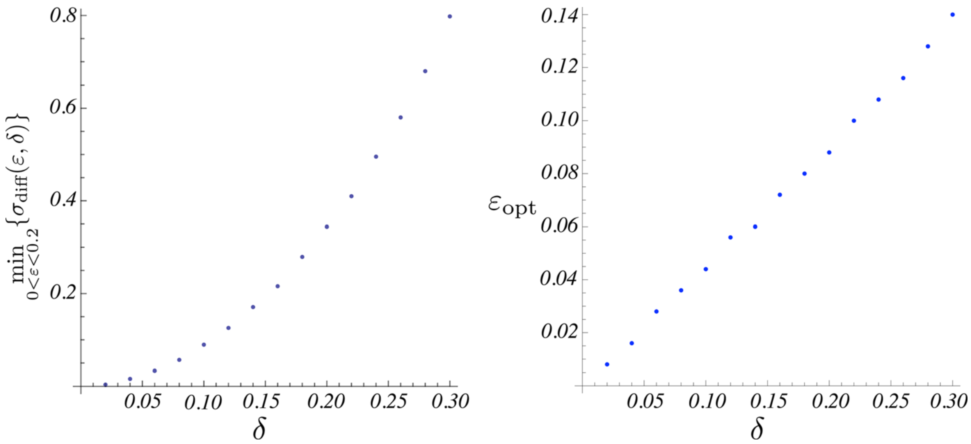

FIG. 11. (Color online) Minimum relative difference between the growth rates of unstable modes in the region $1<\alpha<4$ and $0<J<1$. The region of parameters considered here is defined by $0<\delta<0.3$ and $0<\varepsilon<0.2$. Also shown on the right-hand side are the optimal values of ε for which the minimum relative difference is attained.

and Zhu and Lawrence[16] have used values of $\varepsilon=4\times10^{-4}$ and 1.59×10^{-3}, respectively. However, Pouliquen *et al.*[9] have used larger values of ε, such as $\varepsilon=0.06132$, 0.0755, and 0.08. In all these studies, the Boussinesq approximation has been used to solve analytically the eigenvalue problem, but we will show that a more careful study may be needed in certain conditions.

Holmboe waves have been observed in laboratory experiments with $\delta=0.1$.[16] Suppose that we seek experimentally these waves by using a two-layer fluid configuration for which $\varepsilon=0.045$. One would think that the Boussinesq limit is perfectly valid for this value of ε (since it is less than the values used by Pouliquen *et al.*[9]). However, as shown in Fig. 10, this is far from being true. While the linearized Euler equations predict two unstable modes with comparable growth rates (provided that ε is sufficiently small), neglecting the value of ε could have some serious repercussions on understanding the instability mechanism and estimating the wavelengths and phase speeds.

Finally, to fully use the results without the Boussinesq approximation, we would like to propose tailoring the two-fluid experiment so that the Holmboe waves can be observed more easily. Here, we have restricted our region of parameters to $0<\delta<0.3$ and $0<\varepsilon<0.2$, within the range of previous experiments.

To obtain the numerical results displayed in Fig. 11, we proceed as follows. First, we consider for the region of parameters a grid with 15×50 points uniformly distributed along the δ and ε-axes, respectively. Then, for each grid point, we compute the maximum growth rate curve on the (α, J)-plane region limited by $0<\alpha<4$ and $0<J<1$ and determine at which Richardson number along the curve, the minimum relative difference of growth rates is attained. Naturally, the results can be improved by considering a more refined mesh, but our purpose here is solely to reveal what the general trend is. As δ increases, the relative differences σ_{diff} grow, and the only way of containing this effect—to be able to observe Holmboe waves—is by increasing also the value of ε. This explains why the idea that Holmboe waves can be more easily obtained for smaller values of ε is false. Just to give an example, for $\delta=0.14$ by picking two fluids for which $\varepsilon=4\times10^{-3}$, we would obtain $\sigma_{\text{diff}}\approx0.2254$, which is larger than 0.17085 obtained for $\varepsilon=0.06$.

V. CONCLUDING REMARKS

We have presented the linear stability results for two-layer shear flows with and without the Boussinesq approximation. It is shown how the two results are formally related through a special limit of small ε and their difference increases with ε, as expected. Even for the case of small ε, where the Boussinesq approximation should be a good approximation, it is shown that great care must be made to obtain accurate stability results when the interface is displaced relative to the center of the shear layer. In this paper, we focus primarily on the effects caused by both the density increment in the stratification and the displacement of the density interface, which are measured by ε and δ, respectively.

In the case when $\delta=0$, Holmboe waves are expected to occur for small values of ε, but it is not clear if the phenomenon persists as ε increases. We show that the possibility of Holmboe instability to happen is seriously reduced as ε increases, reaching the stage where Holmboe waves simply cannot exist. This is due to the fact that the maximum growth rate curve on the (α, J)-plane can enter into an unstable region, denoted by $\mathcal{U}$, where only one unstable mode exists.

The presence of $\mathcal{U}$ is even more relevant in the case when $\delta\neq0$, commonly observed in mixing layer facilities. These were long believed to be an effective mean to study Holmboe waves. However, although ε is small in the experiment of Lawrence *et al.*,[13] it has been known that only one-sided instability can be observed both near the splitter plate and at the far downstream of the splitter plate. Near the splitter plate where δ is relatively large, there exist two unstable modes for small J, but their growth rates are so different that only one mode, more unstable than the other, is excited. On the other hand, as J increases, the mode with the maximum growth rate appears in $\mathcal{U}$ (that had not been detected prior to this study) and, therefore, only a single unstable mode is excited, as described earlier. Our results show that most likely, regardless of the magnitude of ε, Holmboe waves cannot be observed if δ is considerably greater than 0.2. Meanwhile, at the far downstream of the splitter plate where δ becomes smaller, two unstable modes have comparable growth rates over only a small range of J, essential for Holmboe instability. This might represent a last hope to this experimental apparatus to study Holmboe waves, as long as J is carefully chosen to fit in that regime at farther downstream.

With a displaced interface of $\delta = 0.1$, Holmboe waves have been observed in exchange flows (cf. Zhu and Lawrence[16]) with small ε of $O(10^{-3})$ for which the Boussinesq approximation should be valid. However, larger values of ε have been also used in previous experiments (e.g., $\varepsilon = 0.08$ in Ref. 9) and it is then legitimate to ask ourselves to which extent the Boussinesq approximation can be used in the linear stability analysis. For this particular value of δ, we have shown that, even for $\varepsilon = 0.045$, the results based on the Boussinesq approximation are inaccurate. The reduced model under the Boussinesq approximation cannot capture the jump along the maximum growth rate curve and, as a result, substantial discrepancies are found with respect to the wavelength, and phase speed, of the unstable features of the system.

ACKNOWLEDGMENTS

This work was partially done when R.B. was visiting the Basque Center for Applied Mathematics as a Postdoctoral Fellow, and he gratefully acknowledges support through Grant No. MTM2008-03541 by the MICINN of Spain. W.C. is supported by the WCU (World Class University) program through the National Research Foundation of Korea funded by the Ministry of Education, Science, and Technology (R31-2008-000-10045-0).

APPENDIX: THE EIGENVALUE EQUATION FOR THE DISPLACED CASE

The eigenvalue Eq. (22) for the configuration setting proposed by Lawrence *et al.*,[13] where the density interface is displaced from the level $z = 0$, is found in dimensionless form as

$$a_0\xi^4 + a_1\xi^3 + a_2\xi^2 + a_3\xi + a_4 = 0, \tag{A1}$$

where the expressions for the coefficients are the following:

$$\begin{aligned}
a_0 &= -\alpha^3(\varepsilon - 2)e^{\alpha(\delta+2)},\\
a_1 &= -\alpha^2 e^{\alpha}\left[2e^{\alpha(\delta+1)}(\alpha\delta(\varepsilon-2)-\varepsilon) + \varepsilon(e^{2\alpha\delta}+1)\right],\\
a_2 &= -\alpha[e^{\alpha(\delta+2)}(\alpha(2J+\alpha(\delta^2-1)(\varepsilon-2)-2\delta\varepsilon+2\varepsilon-4)\\
&\quad + 2-\varepsilon) + (\varepsilon-2)e^{\alpha\delta} + \varepsilon e^{\alpha}(\alpha(2\delta+1)+1)\\
&\quad + \varepsilon e^{\alpha(2\delta+1)}(\alpha(2\delta-1)-1)],\\
a_3 &= 2J\alpha e^{\alpha}(1-e^{2\alpha\delta}) + \varepsilon e^{\alpha}[2-\alpha(\alpha\delta(\delta+2)+2)]\\
&\quad + \varepsilon e^{\alpha(2\delta+1)}[2-\alpha(\alpha\delta(\delta-2)+2)] + 2(\alpha-1)^2 e^{\alpha(\delta+2)}\\
&\quad \times(\alpha\delta(\varepsilon-2)-\varepsilon) - 2e^{\alpha\delta}(\alpha\delta(\varepsilon-2)+\varepsilon),\\
a_4 &= (\alpha-1)^2 e^{\alpha(\delta+2)}[2J+\delta(\alpha\delta(\varepsilon-2)-2\varepsilon)]\\
&\quad + (\alpha-1)e^{\alpha}[e^{2\alpha\delta}(2J+\varepsilon\delta(\alpha\delta-2))+2J\\
&\quad - \varepsilon\delta(\alpha\delta+2)] + e^{\alpha\delta}[2J-\delta(\alpha\delta(\varepsilon-2)+2\varepsilon)].
\end{aligned}$$

We remark that when $\varepsilon = 0$ and $J = 0$, Eq. (A1) can be factorized as

$$(\xi+\delta)^2\left[1 + e^{2\alpha}\left(\alpha^2\xi^2 - (\alpha-1)^2\right)\right] = 0.$$

We have always a double real root $\xi = -\delta$ and, depending on the value of α considered, two additional eigenvalues could be real or purely imaginary. This fact explains why for very small values of ε, the most unstable modes travel at approximately speed 0, for $J \ll 1$, regardless how large the parameter δ is. To understand the effect of the density increment ε alone, we can set $\delta = 0$ and $J = 0$ to obtain

$$\begin{aligned}
&\xi[-e^{2\alpha}\alpha^3(\varepsilon-2)\xi^3 + 2e^{\alpha}(e^{\alpha}-1)\alpha^2\varepsilon\xi^2 + [-1+e^{2\alpha}(\alpha-1)^2]\\
&\quad \times\alpha(\varepsilon-2)\xi - 2\varepsilon[1+e^{\alpha}(\alpha-1)]^2] = 0,
\end{aligned}$$

that has always a simple real root $\xi = 0$. Depending on the value of α considered, we can have three more real, or one real and two complex conjugate, roots. This information can be used to understand the combined effects of the displacement of the density interface relative to the center of the shear layer and the density increment in the stratification at the very earliest stage of the instability mechanism.

1. G. I. Taylor, "Effect of variation in density on the stability of superposed streams of fluid," Proc. Roy. Soc. London, Ser. A **132**, 499 (1931).
2. S. Goldstein, "On the stability of superposed streams of fluids of different densities," Proc. Roy. Soc. London, Ser. A **132**, 524 (1931).
3. J. Holmboe, "On the behaviour of symmetric waves in stratified shear layers," Geophys. Publ. **24**, 67 (1962).
4. P. Hazel, "Numerical studies of the stability of inviscid stratified shear flows," J. Fluid Mech. **51**, 39 (1972).
5. W. D. Smyth, G. P. Klaassen, and W. R. Peltier, "Finite amplitude Holmboe waves," Geophys. Astrophys. Fluid Dyn. **43**, 181 (1988).
6. W. D. Smyth and W. R. Peltier, "The transition between Kelvin-Helmholtz and Holmboe instability: An investigation of the overreflection hypothesis," J. Atmos. Sci. **46**, 3698 (1989).
7. W. D. Smyth and W. R. Peltier, "Three-dimensional primary instabilities of a stratified, dissipative, parallel flow," Geophys. Astrophys. Fluid Dyn. **52**, 249 (1990).
8. A. Alexakis, "On Holmboe's instability for smooth shear and density profiles," Phys. Fluids **17**, 084103 (2005).
9. O. Pouliquen, J. M. Chomaz, and P. Huerre, "Propagating Holmboe waves at the interface between two immiscible fluids," J. Fluid Mech. **266**, 277 (1994).
10. S. A. Thorpe, "A method of producing a shear flow in a stratified fluid," J. Fluid Mech. **32**, 693 (1968).
11. F. K. Browand and C. D. Winant, "Laboratory observations of shear layer instability in a stratified fluid," Boundary-Layer Meteorol. **5**, 67 (1973).
12. C. G. Koop and F. K. Browand, "Instability and turbulence in a stratified fluid with shear," J. Fluid Mech. **93**, 135 (1979).
13. G. A. Lawrence, F. K. Browand, and L. G. Redekopp, "The stability of a sheared density interface," Phys. Fluids A **3**(10), 2360 (1991).
14. G. A. Lawrence, S. P. Haigh, and Z. Zhu, "In search of Holmboe's instability," in *Physical Processes in Lakes and Oceans, Coastal and Estuarine Studies* (AGU, Washington, D.C., 1998), Vol. 54, p. 295.
15. D. Zhu and G. A. Lawrence, "Exchange flow through a channel with an underwater sill," Dyn. Atmos. Oceans **24**, 153 (1996).
16. D. Zhu and G. A. Lawrence, "Holmboe's instability in exchange flows," J. Fluid Mech. **429**, 391 (2001).
17. E. W. Tedford, R. Pieters, and G. A. Lawrence, "Symmetric Holmboe instabilities in a laboratory exchange flow," J. Fluid Mech. **636**, 137 (2009).

[18]P. G. Drazin and W. H. Reid, *Hydrodynamical Stability*, 2nd ed. (Cambridge University Press, Cambridge, 2004).
[19]A. T. Fuller, "Root location criteria for quartic equations," IEEE Trans. Autom. Control. **26**(3), 777 (1981).
[20]E. I. Jury and M. Mansour, "Positivity and nonnegativity conditions of a quartic equation and related problems," IEEE Trans. Autom. Control **26**(2), 444 (1981).
[21]R. Barros and W. Choi, "On the hyperbolicity of two-layer ows," in *Frontiers of Applied and Computational Mathematics* (World Scientific, Singapore, 2008), pp. 95–103.
[22]O. M. Umurhan and E. Heifetz, "Holmboe modes revisited," Phys. Fluids **19**, 084102 (2007).
[23]S. P. Haigh and G. A. Lawrence, "Symmetric and nonsymmetric Holmboe instabilities in an inviscid flow," Phys. Fluids A **11**(6), 1459 (1999).
[24]N. Yonemitsu, "The stability and interfacial phenomena of a salt wedge flow," Ph.D. thesis, University of Alberta, Edmonton, Canada, 1991.
[25]N. Yonemitsu, G. E. Swaters, N. Rajaratnam, and G. A. Lawrence, "Shear instabilities in arrested salt-wedge flows," Dyn. Atmos. Oceans **24**, 173 (1996).
[26]J. R. Carpenter, N. J. Balmforth, and G. A. Lawrence, "Identifying unstable modes in stratified shear layers," Phys. Fluids **22**, 054104 (2010).